Spatiotemporal Genetic Structure of Regional-scale *Alexandrium catenella* Dinoflagellate Blooms explained by Extensive Dispersal and Environmental Selection

Yida Gao[1], Ingrid Sassenhagen[1,4], Mindy L. Richlen[2], Donald M. Anderson[2], Jennifer L. Martin[3] & Deana L. Erdner[1]*

[1]Marine Science Institute, University of Texas at Austin, Port Aransas, TX 78373, USA

[2]Woods Hole Oceanographic Institution, Woods Hole, MA 02543, USA

[3]Fisheries and Oceans Canada, Biological Station, St. Andrews, NB, E5B 0E4, Canada

[4]Laboratoire d'Océanologie et des Geosciences, UMR LOG 8187, Université du Littoral Côte d'Opale, Wimereux, France

*corresponding author: derdner@utexas.edu

Abstract

Paralytic Shellfish Poisoning (PSP) caused by the dinoflagellate *Alexandrium catenella* is a well-known global syndrome that negatively impacts human health and fishery economies. Understanding the population dynamics and ecology of this species is thus important for identifying determinants of blooms and associated PSP toxicity. Given reports of extensive genetic heterogeneity in the toxicity and physiology of *Alexandrium* species, knowledge of genetic population structure in harmful algal species such as *A. catenella* can also facilitate the understanding of toxic bloom development and ecological adaptation. In this study we employed

microsatellite markers to analyze multiple *A. catenella* strains isolated from several sub-regions in the Gulf of Maine (GoM) during summer blooms, to gain insights into the sources and dynamics of this economically important phytoplankton species. At least three genetically distinct clusters of *A. catenella* were identified in the GoM. Each cluster contained representatives from different sub-regions, highlighting the extent of connectivity and dispersal throughout the region. This shared diversity could result from cyst beds created by previous coastal blooms, thereby preserving the overall diversity of the regional *A. catenella* population. Rapid spatiotemporal genetic differentiation of *A. catenella* populations was observed in local blooms, likely driven by natural selection through environmental conditions such as silicate and nitrate/nitrite concentrations, emphasizing the role of short-term water mass intrusions and biotic processes in determining the diversity and dynamics of marine phytoplankton populations. Given the wide-spread intraspecific diversity of *A. catenella* in GoM and potentially elsewhere, harmful algal blooms will likely persist in many regions despite global warming and changing environmental conditions in the future. Selection of different genetic lineages through variable hydrological conditions might impact toxin production and profiles of future blooms, challenging HAB control and prediction of PSP risk in the future.

Keywords

Alexandrium, harmful algal blooms, population structure, dispersal, environmental selection

1. Introduction

Paralytic Shellfish Poisoning (PSP) caused by the dinoflagellate *Alexandrium catenella* is a global issue that negatively impacts human health and fisheries (Hallegraeff, 1993; Van Dolah, 2007). The Gulf of Maine (GoM) is a continental shelf sea located in the northwest Atlantic where a large areas of shellfish resources are recurrently contaminated by PSP (Anderson et al., 2014a). As a consequence, the local commercial and recreational shellfishing industries regularly suffer from seafood safety issues, resulting in a loss of millions of dollars in some years. According to long-term monitoring data, *A. catenella* blooms in the western GoM usually start in late April, peak in June or mid-July with cell densities reaching or exceeding ten thousand cells per liter, and decline in late July (Li et al., 2014; Martin et al., 2014a). The life cycle of *A. catenella* includes an annual alternation between haploid vegetative cells that germinate in response to favorable conditions in early spring, and a resting stage (cyst) that is presumably formed in response to adverse environmental conditions in the field (Anderson et al., 1983; Anderson & Lindquist, 1985; Brosnahan et al., 2015). Previous physiological research on *A. catenella* in GoM revealed that strains from northern areas had higher toxin content and different toxin composition than strains from the south (Anderson et al., 1994; Maranda et al., 1985). Based on these differences in toxicity and other distinctions in bioluminescence and morphology, a northern and a southern cluster of *A. catenella* were proposed (Anderson et al. 1994). However, the dynamics of the population structure of *A. catenella* in GoM are still unclear, limiting our ecological understanding of the development and persistence of harmful algal blooms (HABs) in the region.

In recent years, many population genetics studies have observed spatiotemporal structure in a large variety of marine phytoplankton species (Alpermann et al., 2010; Casabianca et al., 2012; Godhe et al., 2016; Richlen et al., 2012), which have greatly challenged the idea that phytoplankton populations are panmictic. These observed spatial and/or temporal genetic differentiation of phytoplankton populations was attributed to three factors: (1) oceanographic connectivity: physical barriers such as circulation and benthic topography can determine dispersal pathways of planktonic cells, therefore determining the extent of gene flow between phytoplankton populations (Casabianca et al. 2012; Godhe et al. 2013; Sjöqvist et al. 2015); (2) Natural selection: environmental conditions can select for individuals with high fitness, resulting in adaptation of a population to the local environmental conditions and providing a competitive advantage of the native population over migrants (Blanquart et al., 2013; Sjöqvist et al., 2015); and (3) isolation by distance (IBD): gene flow and sexual recombination occur more frequently among geographically-close individuals, so distant populations may diverge due to limited gene flow (Hamilton, 2011).

Most previous studies about population genetics of marine HABs focused on spatial structure of phytoplankton populations across large spatial scales, and connectivity explains many instances of spatial differentiation of marine micro-algal populations (e.g. Nagai et al., 2009; Casabianca et al., 2012; Sjöqvist et al., 2015; Richlen et al., 2012). In addition to spatial structure, temporal differentiation has also been reported in several phytoplankton groups. In diatom populations, temporal genetic structure was linked to silicate depletion (Godhe et al. 2016; Rynearson et al., 2006), possibly indicating local adaptation. In dinoflagellate populations, temporal genetic differentiation of *Gambierdiscus caribaeus* in the Greater Caribbean Region was likely affected

92 by salinity and benthic coverage of the habitat (Sassenhagen et al., 2018). Temporal population
93 structure has also been examined in the genus *Alexandrium*. Dia et al. (2014) monitored the
94 temporal population differentiation of the dinoflagellate *Alexandrium minutum* in two estuaries
95 in France and showed that interannual genetic differentiation was greater than intra-bloom
96 differentiation. Temporal differentiation in blooms of the dinoflagellate *A. catenella* in salt ponds
97 near GoM was observed to occur on short (< 1 month) time scales, potentially driven by different
98 timing of excystment, parasitism and grazing (Richlen et al., 2012). During the *Alexandrium*
99 bloom in GoM in the year 2005, temporal succession of two genetically distinct sub-populations
100 was observed on similar time scales (Erdner et al., 2011).
101
102 In this study, we investigated the genetic dynamics of *Alexandrium catenella* blooms in the GoM
103 by sampling over three summer months in 2007, from several sub-regions, providing good
104 spatial coverage of the blooms. The main objectives of this investigation were to: (1) examine
105 temporal changes in genetic composition during local *A. catenella* blooms in the GoM; (2)
106 determine the regional genetic structure and sources of *A. catenella* populations across the GoM;
107 and (3) test associations between environmental conditions and genetic differentiation. Based on
108 previous research we hypothesized that barriers to panmixia (e.g. hydrography) may weaken
109 gene flow between northern and southern regions of the GoM and facilitate the formation of
110 spatially-differentiated *A. catenella* sub-populations. Natural selection of adapted genotypes may
111 cause short-term temporal genetic differentiation during local blooms in the GoM. By using
112 microsatellite markers on *A. catenella* strains we sought to reveal the sources and dynamics of
113 this economically important phytoplankton species in the GoM, providing insights for future
114 bloom sustainability and toxicity under global warming and changing environmental conditions.

115

116 **2. Method**

117 2.1 Study sites

118 Bloom sampling focused on three sub-regions within the GoM area (Figure 1): Georges Bank
119 (GB), Bay of Fundy (BoF) and Nantucket Shoal (NS). GB is characterized by a central bank,
120 which is 60 meters deep and influenced by a strong clockwise gyre that retains water as long as
121 90 days (Brink et al., 2003). The BoF is characterized by extensive local cyst beds, a retentive
122 hydrography (e.g. gyre), and regular nutrient inflow from tidal water masses (Anderson et al.,
123 2014b; Martin et al., 2014a). NS is a submerged, shallow, sand and gravel ridge that acts as a
124 topographic barrier to deep flow between the GoM and the New England continental shelf
125 (Limeburner & Beardsley, 1982). The Main Coastal Current (MCC; Pettigrew et al., 2005) and
126 the Gulf of Maine Coastal Plume (Keafer et al., 2005) are the dominant currents in the GoM, and
127 they flow from the BoF in the Northeast to southern parts of the Gulf (Figure 1).

128

129 2.2 Sampling

130 In May 2007, an *A. catenella* bloom covered most parts of GB with cell concentrations up to
131 12,000 cells L^{-1}, and then declined in June with advection to NS (McGillicuddy et al., 2014). In
132 contrast, the inshore bloom along the BoF did not develop until June, after the GB bloom had
133 traveled to NS (Martin et al., 2014b; McGillicuddy et al., 2014).

134

135 The *A. catenella* blooms in the surface water (0-1 m depth) were sampled at several stations in
136 GB, BoF and NS during cruises EN435 and 437 in 2007 (Figure 1). Sampling dates and number
137 of strains per sample were shown in Table 1. Eleven samples at GB (GBA-GBK), eight samples

in BoF (BFA-BFH), and three samples in NS (NSA-NSC) were collected during the bloom season. GB samples were taken around the shallow central bank from late May to early July. Strains from GBB&GBH and GBD&GBK were obtained from the exactly same locations (Figure 1). Among BoF samples, BFC and BFF were taken during cruises, while other samples were taken from field work by Jennifer Martin. BFA, BFD and BFH were sampled from Passamaquoddy Bay, while BFG was collected near the Wolves Islands, and BFB and BFE were pooled samples from Passamaquoddy Bay and the Wolves Islands. Single *A. catenella* cells were isolated by micropipette and cultured in 96-well plates as in Erdner et al., 2011. A total of 761 clonal strains were established for this study, representing 18-40 clonal strains from each sample.

2.3 DNA extraction and microsatellite genotyping

In order to extract DNA, each clonal culture was harvested when the cell density exceeded 100 cells per well. DNA was extracted from 200 µL of each culture using the Generation Capture Column Kit (Qiagen, Valencia, CA) following the manufacturer's instructions. From the thirteen microsatellite loci found by Nagai et al. (2004), the four loci Atama 15, Atama 23, Atama 27 and Atama 39 were selected for this study based on amplification success and the observed number of alleles. These same microsatellite markers have previously been employed to examine the genetic diversity and differentiation of *A. catenella* populations sampled in 2005 to 2007 from the GoM and Nauset Estuary on Cape Cod, MA, USA (Erdner et al., 2011; Richlen et al., 2012). PCR reactions contained ~5 ng of template DNA, 0.2mmol L^{-1} of each dNTP, 0.5 µmol L^{-1} of each designed primer pair, with one primer labeled with 6FAM, NED, PET, or VIC, 1x PCR buffer (10mmol L^{-1} Tris-HCl, pH 8.3, 500 mmol L^{-1} KCl, 15 mmol L^{-1} $MgCl_2$, 0.01% w/v gelatin), and 0.25 U of Ampli Taq Gold (Applied Biosystems, Foster City, CA), in 10 µL total

volume. The PCR cycling conditions were as follows: 10 min at 94 °C, 10 cycles of 30 sec at 94°C, 30 sec at 60°C and 1 min at 72°C, and then 28 cycles of 30 sec at 94°C, 30 sec at the primer-specific annealing temperature (Nagai et al., 2004), and 1 min at 72°C, and a final elongation for 5 min at 72°C. In order to determine if amplification was successful, PCR products were run on a 1% TAE agarose gel. For allele size analysis, PCR products were diluted 3-5x with nuclease-free water, and 1 µL of diluted product was mixed with 0.25 µL 500 LIZ Size Standard and 8.75 µL Hi-Di Formamide, and then analyzed using an ABI 3730xi DNA Analyzer (Applied Biosystems, Foster City, CA). Allele sizes were determined using the program FPMiner (2005; Bioinfor-Soft LLC, Beaverton, OR). Microsatellite data is available from the Mendeley Data repository, doi: 10.17632/nhwkm3nczj.1.

2.4 Microsatellite Data Analysis

2.4.1 Genetic diversity

Allele diversity (Nei 1973) was calculated based on all individuals as well as only unique genotypes in each genetic sub-cluster using POPGENE v. 1.32 (Yeh et al., 1997). Clonal diversity was defined as the ratio of the number of unique four-locus genotypes (G) to the total number of genotypes analyzed (N) with a threshold of one base to distinguish clones in Arlequin v. 3.5.1.2 (Excoffier et al., 2005). This parameter was also calculated after adjusting the sample size of each genetic sub-cluster to N=59 by using the R function “sample”. Multilocus linkage disequilibrium was assessed by the Monte Carlo method in LIAN v. 3.5 with 10,000 resamplings (Haubold & Hudson, 2000), while linkage disequilibrium between pairs of loci was determined in GenePop v. 4.5 with Markov Chain parameters of 1000 dememorisation steps and 100 batches with 1000 iterations per batch (Rousset et al., 2008).

184

185 2.4.2 Inference of population structure

186 To identify the genetic clusters in the GoM dataset, PCAGEN was applied to run a principal
187 components analysis (PCA) based on allele frequencies, with 10000 randomisations used to
188 determine the significance of the inertia of each axis (Goudet, 1999).

189

190 Genetic composition and structuring were examined using Bayesian cluster analysis
191 implemented in STRUCTURE 2.3.2 (Pritchard et al., 2000). The number of potential clusters (K)
192 was first assessed using 10 runs performed at every K value from 1 to 10, each with a burn-in
193 period of 100,000 steps and 200,000 Markov Chain Monte Carlo repetitions. Simulations were
194 conducted using the admixture model with the locprior option, assuming correlated allele
195 frequencies among populations. The calculation of the most likely value of K was performed in
196 Structure Harvester Web v0.6.94 (Earl, 2012) by the method of ad hoc statistic $\triangle$ K (Evanno et
197 al., 2005).

198

199 The partitioning of genetic variance within and among genetic clusters was assessed using the
200 analysis of molecular variance (AMOVA) implemented in the software GenoDive 2.0b27
201 (Meirmans & Van Tienderen, 2004).

202

203 Genetic clustering of *A. catenella* populations in the GoM was further examined by performing
204 pairwise comparisons. Wright's F_{ST} (Wright, 1949) was used to identify fixation of genetic
205 differences, calculated in Arlequin v. 3.5.1.2 with 10,000 permutations to test for significance.
206 The Fisher's exact test (Raymond, 1995) was used to assess differences in allele frequencies

between clusters, performed in GenePop v. 4.5 using Markov Chain parameters of 1000 dememorisation steps and 100 batches with 1000 iterations per batch (Rousset et al., 2008). All p-values were Bonferroni corrected to account for multiple comparisons.

2.5 Environmental effects

Environmental data were obtained from http://grampus.umeoce.maine.edu/gomtox/gomtox.htm. We included nitrate and nitrite concentrations (µM), temperature (°C), salinity, water density anomaly measured as δT (kg m^{-3}), ammonium (µM), chlorophyll a (µg L^{-1}), phaeopigments (µg L^{-1}), silicate (µM) and phosphate (µM) from surface water of a subset of the same sampling stations as used for isolation of algal strains (GBA, GBB, GBC, GBD, GBE, GBG, GBH, GBJ, GBK and BFC) (Table 2). Environmental data were not available from the other stations, and therefore could not be included in this analysis.

To understand the impact of environmental conditions on the population structure of *A. catenella*, the relationship between genetic structure and environmental variables was tested using a distance based redundancy analysis (dbRDA) (Legendre & Andersson, 1999). Distances between samples based on the genetic data were calculated with a principal coordinate analysis (PCoA) using the R package adegenet 1.0.1 (Jombart, 2008). The relationship between the coordinates of samples from the PCoA and the environmental variables was determined by dbRDA using the R package vegan 2.4-1 (Oksanen et al., 2016).

3. Results

3.1 Genetic differentiation and population dynamics

230 In this study, 761 isolates were genotyped using four different microsatellite loci. Strains that had
231 any null alleles were removed from the data set, resulting in a final set of 667 individuals. All
232 four loci were polymorphic in all samples. There were 158 unique genotypes in the entire data
233 set resulting in an overall clonal diversity of 0.23. Multilocus linkage disequilibrium was not
234 detected ($I_A{}^S$=0.0069, p=0.179), nor was linkage disequilibrium between pairs of loci.
235
236 The *A. catenella* populations displayed more rapid and complicated differentiation over the
237 course of the 2007 blooms compared with the temporal succession from early to late sub-
238 populations as observed in the 2005 bloom across the GoM (Erdner et al., 2011). To identify
239 genetic structure of *A. catenella* populations in the GoM, PCA implemented in the program
240 PCAGEN was performed (Figure 2). The first two axes of the PCA were both significant and
241 explained 38% and 30% of the total variation in F_{ST}, respectively. Three clusters of samples were
242 identified: (1) GBB, GBF, GBG, GBH, GBI, GBK, BFA, BFE, NSA, NSB and NSC (orange
243 samples in Figure 2); (2) GBC, BFC, BFD and BFF (blue samples in Figure 2); (3) BFB, GBJ,
244 GBD and GBE (yellow samples in Figure 2). However, GBA, BFG and BFH (black samples in
245 Figure 2) were in a transitional location between two of the clusters. In order to further examine
246 the genetic differentiation among these three samples, the clustering pattern was investigated
247 using an AMOVA. When GBA was added to Cluster (1) and BFH&BFG were added to Cluster
248 (2), differentiation among clusters was significant (Rct=0.022, p=0.008), but not significant
249 within each cluster (Rsc=0.009, p=0.122). Other grouping patterns were also tested but were less
250 supported by AMOVA based on distribution of within-cluster variation and among-cluster
251 variation (data not shown). The PCA and AMOVA analyses indicated differentiation of the GoM
252 dataset into three genetic clusters based on their genetic similarity, and they were re-named by

253 the location of the majority of samples: (1) **Southern Cluster**: GBA, GBB, GBF, GBG, GBH,
254 GBI, GBK, BFA, BFE, NSA, NSB and NSC; (2) **Northern Cluster:** GBC, BFC, BFD, BFF,
255 BFG and BFH; (3) **Mixed Cluster:** GBD, GBE, GBJ and BFB. These genetic clusters were not
256 entirely grouped according to geography, but instead comprised samples from different sub-
257 regions in the GoM.
258
259 Bayesian analyses implemented in the program STRUCTURE were performed to examine the
260 genetic composition and the relationships of samples (Figure 3). A K value of three was
261 identified as the most likely number of "ancestral" populations in the GoM dataset using the
262 Evanno method. The result of the STRUCTURE bar plot from "K=3" was similar to the "three-
263 cluster" pattern described above, i.e. samples with similar proportional ancestry membership
264 corresponded to the groupings identified by PCA and AMOVA. Subtle population structure was
265 apparent within clusters. BFC's unique genetic composition in STRUCTURE analysis was
266 reflected in its divergence in the PCA plot. The transitional locations of BFG and BFH in PCA
267 analysis were also shown in STRUCTURE with mixed ancestral populations.
268
269 Pairwise F_{ST} values were calculated between the Northern, Southern and Mixed Clusters. All
270 pairwise F_{ST} values between the genetic clusters were significant and ranged from 0.051 to 0.088
271 (Table 3). Additionally, the degree of differentiation based on Fisher's exact test was highly
272 significant between these clusters. Allele frequencies from each genetic cluster were compared in
273 detail. All loci in Southern and Northern Clusters had private alleles, whereas none were
274 observed the Mixed Cluster. For example, of the 21 alleles detected at locus Atama15 in GoM, 8
275 alleles were found only in Southern Cluster while another 4 were found only in Northern Cluster.

In order to understand the sources of the observed genetic differentiation, F_{ST} values based on each locus were calculated (data not shown). The divergence between Southern and Northern Cluster was driven by locus Atama27, as the differentiation was not significant based on other microsatellites loci. Specifically, allele size 162 (87%) was most common in Southern Cluster while allele sizes 162 (56%) and 160 (38%) dominated in Northern Cluster. All loci except Atama 39 were the driving force to differentiate Northern and Mixed Cluster, while only Atama 15 and Atama23 contributed significantly to the genetic differentiation between Southern and Mixed Cluster.

Within sub-regions of the GoM, significant changes in genetic composition were observed during local blooms. GB samples contained representatives from all of the three genetic clusters defined above: (1) GB-Southern: GBA, GBB, GBF, GBG, GBH, GBI and GBK; (2) GB-Mixed: GBD, GBE and GBJ; and (3) GB-Northern: GBC. The pairwise F_{ST} analysis was repeated for the sub-clusters in GB to clarify local population structure. The results confirmed the significant differentiation of this local bloom into the three distinct sub-clusters, with F_{ST} values ranging from 0.058 to 0.134 (data not shown). To gain insights into temporal structure of the GB bloom, **early** (5/26-5/30: GBA, GBB, GBC, GBD and GBE) and **late samples** (6/16-7/3: GBF, GBG, GBH, GBI, GBJ and GBK) were investigated separately. During the early bloom period, all three genetically distinct sub-clusters described above were represented: (1) GB-Southern: GBA and GBB; (2) GB-Northern: GBC; (3) GB-Mixed: GBD and GBE. Pairwise F_{ST} comparisons among sub-clusters that included only samples from the early bloom confirmed patchy distribution of spatially differentiated clusters over the bank during this period, with F_{ST} values ranging from 0.047 to 0.137. Twenty days later, during the late bloom period, a more homogenous distribution

299 of *A. catenella* was observed, as all samples were identified as GB-Southern except GBJ (GB-
300 Mixed).
301
302 BoF samples also contained all three genetic clusters based on the results of PCA and AMOVA
303 analyses of the entire data set: (1) BF-Southern: BFA and BFE; (2) BF-Mixed: BFB; and (3) BF-
304 Northern: BFC, BFD, BFF, BFG and BFH. The pairwise F_{ST} analysis was repeated for the BoF
305 dataset, and indicated significant differentiation of these three sub-clusters, with F_{ST} values
306 ranging from 0.029 to 0.058.
307
308 The genetic diversity of different sub-clusters varied, however (Table 4). The Southern sub-
309 clusters from each sub-region exhibited the lowest Ht: GB (Ht=0.49) and BoF (Ht=0.47).
310 However, the lowest values of Ht (unique) in the respective sub-regions were found in GB-
311 Northern and BoF-Mixed. When strain numbers were equalized to 59, clonal diversity was
312 higher in GB-Mixed (0.63), and distinctly lower in GB-Southern (0.46) among all sub-regions.
313
314 3.2 Environmental Correlation
315 Nine environmental factors were collected from ten samples in the GoM. Some samples stood
316 out due to relatively high nutrient concentrations: GBC with 1.47 µM of nitrate and nitrite; GBD
317 with relatively high silicate concentrations (10.53 µM); and BFC with 6.63 µM of silicate and
318 10.17 µM of nitrate and nitrite (Table 2).
319
320 The impact of variable environmental conditions on the population genetic structure of *A.*
321 *catenella* populations was assessed using a distance-based redundancy analysis (dbRDA).
322 Among nine environmental variables, only silicate (P=0.0068), and nitrate and nitrite (P=0.0007)

concentrations emerged as factors that were significantly associated with the genetic structure (Figure 4). Silicate concentration distinguished GBD and GBE (Mixed Cluster) from the other samples, while nitrate and nitrite concentration primarily drove the divergence of GBC and BFC (Northern Cluster), although the silicate concentration in BFC was also comparatively high.

4. Discussion

This study investigated regional population genetic structure of *A. catenella* blooms distributed throughout the GoM. Spatiotemporal genetic differentiation of *A. catenella* populations was analyzed to describe the dispersal of *A. catenella* cells in the GoM as well as the influence of environmental conditions on their population structure. At least three genetically distinct clusters of *A. catenella* were identified in the GoM based on PCA analysis, STRUCTURE plots, fixation indices of genetic differentiation, and AMOVA. Significant short-term temporal and spatial differentiation was observed within local blooms, and linked to environmental conditions. Across the region as whole, representatives of the three genetic clusters were detected at all locations, indicating significant gene flow that could arise from hydrographic connectivity and the presence of resting (cyst) stages.

Circulation around GB is characterized by a strong gyre that is expected to homogenize *A. catenella* bloom populations, however, small-scale spatial differentiation into several sub-clusters was observed throughout the bloom on this bank. The early bloom period was characterized by three spatial sub-clusters, while the late bloom period was mostly characterized by one homogeneous population. This spatiotemporal variation in population structure at GB may be influenced by many factors, among which nitrate, nitrite and silicate concentrations may

play a key role (Figure 4). During most of the bloom season in GB, abundant and stable supplies of ammonium and phosphate as well as low supply of nitrite and nitrate were found all over the bank (McGillicuddy et al. 2014; Townsend et al. 2014), which coincided with the presence of GB-Southern Cluster. Hence, the *A. catenella* cells from GB-Southern Cluster were likely utilizing ammonium instead of nitrite or nitrate as primary nitrogen source. However, GB-Northern Cluster, located at the Northeast Peak of GB, coincided with significantly higher nitrite and nitrate concentrations, which may have been derived from an inflow of nitrate and nitrite-rich deeper water masses, i.e. Warm Slope Water, onto the Bank along the Northern Flank and Northeast Peak (Hu et al., 2008). Since laboratory experiments have shown differential preference of *A. tamarense* strains for different nitrogen sources (Leong et al., 2004), high nitrite and nitrate concentrations may select for distinct *Alexandrium* strains, facilitating the prevalence of the selected alleles. Occasional increases in silicate concentration on GB may also indirectly select GB-Mixed genotypes, some of which were present at the beginning of the *A. catenella* bloom in early summer, co-existing and likely competing with the annual spring diatom bloom (Townsend et al., 2014). This distribution pattern of silicate may result from regeneration of silicate from diatom frustules produced in spring bloom (Gettings et al., 2014). Short-term variations in nutrient concentrations may thus have rapidly selected for distinct genotypes, which were present before in low concentrations, and disrupted the otherwise homogenous population structure at GB. Many previous studies have described the effect of natural selection on the change of genetic structure within short periods (Rynearson et al., 2006; Godhe et al., 2016; Sassenhagen et al., 2018). For example, changes in environmental conditions such as salinity could rapidly select favorable genotypes and therefore drive genetic differentiation of *Gambierdiscus caribaeus* in the Greater Caribbean Region (Sassenhagen et al., 2018).

Succession of genetically distinct populations of the diatom *Skeletonema marinoi* was observed even within fifteen days after a decline in silicate concentrations in the Baltic Sea (Godhe et al., 2016).

NS samples were not genetically different from the dominant cluster on GB (GB-Southern), thus strong algal dispersal and gene flow strengthened by the Gulf of Maine Coastal Plume (Keafer et al., 2005) or other currents might occur between these two sub-regions. Stable genetic composition of the *A. catenella* population in NS during the sampling period may reflect overall stable local environmental conditions. However, since no information about the NS cyst bed and transport through sub-subface layers are available, the sources of NS populations still need to be explored.

The BoF is considered to retain phytoplankton cells through the Minas Basin cyclonic gyre (Aretxabaleta et al., 2009; Townsend et al., 2014) and an extensive cyst seedbed (Anderson et al., 2014b; Martin et al., 2014a), potentially restricting gene flow yet preserving high genetic diversity of algal species (Sundqvist et al., 2018). Our results showed significant temporal genetic differentiation in the BoF among samples collected at roughly the same location. This pattern may result from induction of sexual reproduction by unfavorable conditions. In *Alexandrium*, environmentally induced encystment could strengthen the effects of natural selection on dominant genotypes by removing lineages that are less successful under the prevailing conditions. At the same time, some genotypes will be favored and accelerate vegetative growth. This characteristic would facilitate the domination of the population by a few successful lineages, effectively reducing gene flow between sub-clusters (Erdner et al., 2011).

392 The turnover rates of genetically distinct sub-clusters were as short as seven days in the BoF.
393 Such rapid changes in population structure may facilitate the persistence of phytoplankton
394 populations in variable marine environments (Rynearson & Armbrust, 2005). Temporal
395 differentiation of phytoplankton populations has been observed in several different microalgal
396 species from many locations around the world (Godhe et al. 2016; Richlen et al. 2012;
397 Rynearson & Armbrust, 2005). In particular, rapid (~one week) temporal differentiation in
398 populations of the dinoflagellate *A. catenella* was also observed in Cape Cod MA (USA) salt
399 pond systems, which may have been facilitated by early induction of sexuality and different
400 timing of germination that preserved the genetic diversity of local populations (Richlen et al.,
401 2012).
402
403 Environmental data were unfortunately not available from most samples from BoF for
404 correlation analysis with the observed population structure. The only sample with available
405 environmental data (BFC) was characterized by much higher nitrate and nitrite conditions – as
406 was GBC – which might have selected for comparatively similar genotypes in both locations.
407 Thus, variable nutrient concentrations might have induced the observed rapid temporal genetic
408 differentiation of *A. catenella* populations in the BoF throughout the sampling period, which
409 could have been facilitated by local cyst beds with high genotype diversity. In order to test this
410 hypothesis, further research should be directed to investigating the genetic diversity of the resting
411 cysts in the BoF.
412
413 Although GB and the BoF are located at the southern and northeastern regions of the GoM
414 respectively, at least 400 km apart from each other, several samples from both sites were very

similar to each other genetically and belonged to the same clusters, which may indicate algal dispersal across the region. Studies of the population genetic structure of the dinoflagellate *Cochlodinium polykrikoides* across the Sea of Japan found evidence for strong dispersal and gene flow over a distance of more than 600 km, highlighting the important role of Tsushima Warm Current on the connectivity of algal populations (Nagai et al., 2009). The BoF is located upstream of the MCC, the prevailing current that flows from Northeast to southern parts of the Gulf, and the bloom in BoF is supported by an extensive local cyst bed and a retentive gyre at the mouth of the Bay. The gyre is leaky, however (Aretxabaleta et al., 2009), so there is potential for dispersal from this northern area to affect the initiation and genetic structure of distant GB blooms, for example through the transport of vegetative cells from BoF to GB during the bloom.

However, the bloom on GB was extensive in May 2007 when there was near absence of *A. catenella* in the coastal waters of the GoM including BoF (McGillicuddy et al., 2014). Furthermore, during the bloom season of that year no evidence of *A. catenella* cells was found in surface waters between Casco Bay and Cape Cod, which is the main circulation pathway connecting BoF and GB-NS (McGillicuddy et al., 2014). Additionally, Li et al. (2014) studied coastal ocean connectivity in the GoM using surface numerical particle tracking and found that the circulation significantly retained particles within the BoF in 2007. As the gyre-like circulation in the BoF may serve as a barrier reducing surface connectivity between BoF and south-western parts of the GoM in 2007, surface cells from the BoF may not be the source of cells blooming on GB. However, the transport of cells through sub-surface layers between the BoF and GB cannot be excluded due to a lack of information about this process.

438 Other potential explanations for observed patterns of genetic connectivity could be the formation
439 of cyst beds on GB or inshore areas including BoF and mid-coast Maine (Anderson et al., 2014b)
440 that contained a mix of resting stages from different genetic clusters. During summer 2005, the
441 GoM experienced the largest *A. catenella* bloom in the preceding three decades, spanning over
442 700 km of coastline. In that year, temporal succession of different inshore *A. catenella* sub-
443 populations was observed during the bloom (Erdner et al., 2011). These differentiated blooms
444 could have resulted in the formation of cysts with high genotype diversity, allowing rapid
445 changes in population structure through natural selection of germinating cells. Although the
446 bloom in 2006 was smaller than in other years, numerical simulations showed a significant
447 number of particles traveling from BoF to the western GoM that year (Li et al., 2014), which
448 may have further enhanced genetic diversity in the downstream cyst beds. Similarly, low to
449 moderate algal dispersal via the MCC across the GoM over many years might have contributed
450 to mixed cysts beds throughout the region.
451
452 Previous studies have found significant numbers of *A. catenella* cysts in benthic nepheloid layers
453 (BNLs) throughout the GoM, representing a deep interconnection between BoF, MCC and south-
454 central regions of the gulf (Pilskaln et al., 2014). Resuspended cysts may therefore serve as
455 bloom inoculum on GB. Although cyst concentrations in the sediments of GB were roughly two
456 orders of magnitude smaller than in the coastal GoM (Anderson et al., 2014b; McGillicuddy et
457 al., 2014), local germination might still contribute at least partially to the bloom on GB.
458 Furthermore, even low cyst concentrations might be sufficient for inoculation of a bloom due to
459 rapid exponential growth of microalgae under favorable environmental conditions. McGillicuddy
460 et al. (2014) also hypothesized that cysts could be transported to the bank from the adjacent deep

461 basins by tidal pumping. Our results suggest significant dispersal and gene flow throughout the
462 GoM, resulting in the absence of endemic populations. Meanwhile, the results described herein
463 also highlight the need for a comprehensive cyst bed investigation including cyst abundance,
464 genetic diversity and transport pathway across the GoM.
465
466 **5. Conclusions**
467 At least three genetically distinct clusters of *A. catenella* were identified in the GoM. Each
468 cluster contains representatives from different sub-regions, highlighting the extent of
469 connectivity and dispersal throughout the GoM. This shared diversity could result from cyst beds
470 containing a mix of resting stages from different genetic clusters. The cyst beds would preserve
471 the overall diversity of the regional *A. catenella* population and allow selection of
472 physiologically and phenotypically different genotypes based on local conditions. Rapid
473 temporal and spatial genetic differentiation of *A. catenella* populations, as observed in local
474 blooms, was likely associated with natural selection through environmental conditions such as
475 silicate and nitrate/nitrite concentrations, emphasizing an important role of the changing nutrient
476 environment in determining the diversity and dynamics of marine phytoplankton populations.
477 This observed short-term genetic differentiation may be indicative of patchiness of different
478 water masses and biotic processes during the development of the bloom. Given the wide-spread
479 intraspecific diversity of *A. catenella* in the GoM and potentially elsewhere, blooms of this
480 species will likely persist in many regions despite global warming and changing environmental
481 conditions in the future. Furthermore, selection of different genetic lineages through variable
482 environmental conditions might impact toxin production and profiles of future blooms,

challenging HAB control and prediction of PSP risk with changeable toxicity effect and persistent bloom dynamics.

6. Acknowledgement

We thank David Townsend for collection and provision of environmental data of sampling stations, and Bruce Keafer, Kerry Norton and Dave Kulis for their hard work in obtaining the samples used in this study. We also gratefully acknowledge the work of captains and crews of the R/V Endeavor. This study was supported by National Science Foundation [grant numbers OCE-0430724, OCE-0850421, OCE-0911031, OCE-1314642, OCE1840381] and National Institutes of Health [grant numbers 1P50-ES012742-01, 1P50-ES021923-01, and 1P01-ES028938-01] through the Woods Hole Center for Oceans and Human Health. Funding was also provided by NOAA Grant [NA06NOS4780245, NA11NOS4780061 and NA15NOS4780181]. This is contribution *** from the US ECOHAB program.

Author Contributions

DLE, MLR, and DMA conceived and designed the work; YG, IS, DLE, MLR, and JLM acquired, analyzed, and/or interpreted the data; YG and IS drafted the work; and all authors provided critical revision for important intellectual content.

506
507
508
509
510
511
512
513

References

515

516 Alpermann, T. J., Tillmann, U., Beszteri, B., Cembella, A. D., & John, U. (2010).
517 PHENOTYPIC VARIATION AND GENOTYPIC DIVERSITY IN A PLANKTONIC
518 POPULATION OF THE TOXIGENIC MARINE DINOFLAGELLATE ALEXANDRIUM
519 TAMARENSE (DINOPHYCEAE)1. *Journal of Phycology*, *46*(1), 18–32.
520 Anderson, D. M., Chisholm, S. W., & Watras, C. J. (1983). Importance of life cycle events in the
521 population dynamics of Gonyaulax tamarensis. *Marine Biology*, *76*(2), 179–189.
522 Anderson, D. M., Couture, D. A., Kleindinst, J. L., Keafer, B. A., McGillicuddy, Jr., D. J.,
523 Martin, J. L., … Solow, A. R. (2014a). Understanding interannual, decadal level variability
524 in paralytic shellfish poisoning toxicity in the Gulf of Maine: The HAB Index. *Deep Sea*
525 *Research Part II: Topical Studies in Oceanography*, *103*, 264–276.
526 Anderson, D. M., Keafer, B. A., Kleindinst, J. L., McGillicuddy, D. J., Martin, J. L., Norton,
527 K., … Butman, B. (2014b). Alexandrium fundyense cysts in the Gulf of Maine: Long-term
528 time series of abundance and distribution, and linkages to past and future blooms. *Deep Sea*

529 *Research Part II: Topical Studies in Oceanography*, *103*, 6–26.
530 Anderson, D. M., Kulis, D. M., Doucette, G. J., Gallagher, J. C., & Balech, E. (1994).
531 Biogeography of toxic dinoflagellates in the genus Alexandrium from the northeastern
532 United States and Canada. *Marine Biology*, *120*(3), 467–478.
533 Anderson, D. M., & Lindquist, N. L. (1985). Time-course measurements of phosphorus
534 depletion and cyst formation in the dinoflagellate Gonyaulax tamarensis Lebour. *Journal of*
535 *Experimental Marine Biology and Ecology*, *86*(1), 1–13.
536 Aretxabaleta, A. L., McGillicuddy, D. J., Smith, K. W., Manning, J. P., & Lynch, D. R. (2009).
537 Model simulations of the bay of fundy gyre: 2. Hindcasts for 2005-2007 reveal interannual
538 variability in retentiveness. *Journal of Geophysical Research: Oceans*, *114*(9), 1–15.
539 Blanquart, F., Kaltz, O., Nuismer, S. L., & Gandon, S. (2013). A practical guide to measuring
540 local adaptation. *Ecology Letters*, *16*(9), 1195–1205.
541 Brink, K. H., Limeburner, R., & Beardsley, R. C. (2003). Properties of flow and pressure over
542 Georges Bank as observed with near-surface drifters. *Journal of Geophysical Research*,
543 *108*(C11), 8001.
544 Brosnahan, M. L., Velo-Suárez, L., Ralston, D. K., Fox, S. E., Sehein, T. R., Shalapyonok,
545 A., … Anderson, D. M. (2015). Rapid growth and concerted sexual transitions by a bloom
546 of the harmful dinoflagellate Alexandrium fundyense (Dinophyceae). *Limnology and*
547 *Oceanography*, *60*(6), 2059–2078.
548 Casabianca, S., Penna, A., Pecchioli, E., Jordi, A., Basterretxea, G., & Vernesi, C. (2012).
549 Population genetic structure and connectivity of the harmful dinoflagellate Alexandrium
550 minutum in the Mediterranean Sea. *Proceedings of the Royal Society B: Biological Sciences*,
551 *279*(1726), 129–138.

552 Dia, A., Guillou, L., Mauger, S., Bigeard, E., Marie, D., Valero, M., & Destombe, C. (2014).
553 Spatiotemporal changes in the genetic diversity of harmful algal blooms caused by the toxic
554 dinoflagellate Alexandrium minutum. *Molecular Ecology*, *23*(3), 549–560.
555 Earl, D. A. (2012). STRUCTURE HARVESTER: a website and program for visualizing
556 STRUCTURE output and implementing the Evanno method. *Conservation Genetics*
557 *Resources*, *4*(2), 359–361.
558 Erdner, D. L., Richlen, M., McCauley, L. A. R., & Anderson, D. M. (2011). Diversity and
559 Dynamics of a Widespread Bloom of the Toxic Dinoflagellate Alexandrium fundyense.
560 *PLoS ONE*, *6*(7), e22965.
561 EVANNO, G., REGNAUT, S., & GOUDET, J. (2005). Detecting the number of clusters of
562 individuals using the software structure: a simulation study. *Molecular Ecology*, *14*(8),
563 2611–2620.
564 Excoffier, L., Laval, G., & Schneider, S. (2005). Arlequin (version 3 . 0): An integrated
565 software package for population genetics data analysis, 47–50.
566 Gettings, R. M., Townsend, D. W., Thomas, M. A., & Karp-Boss, L. (2014). Dynamics of late
567 spring and summer phytoplankton communities on Georges Bank, with emphasis on
568 diatoms, Alexandrium spp., and other dinoflagellates. *Deep-Sea Research Part II: Topical*
569 *Studies in Oceanography*, *103*, 120–138.
570 Godhe, A., Egardt, J., Kleinhans, D., Sundqvist, L., Hordoir, R., & Jonsson, P. R. (2013).
571 Seascape analysis reveals regional gene flow patterns among populations of a marine
572 planktonic diatom. *Proceedings of the Royal Society B: Biological Sciences*, *280*(1773),
573 20131599–20131599.
574 Godhe, A., Sjöqvist, C., Sildever, S., Sefbom, J., Harðardóttir, S., Bertos-Fortis, M., … Kremp,

575 A. (2016). Physical barriers and environmental gradients cause spatial and temporal genetic
576 differentiation of an extensive algal bloom. *Journal of Biogeography*, *43*(6), 1130–1142.
577 Goudet, J. (1999). PCA-GEN for Windows, V. 1.2. *Institute of Ecology, Univ. of Lausanne.*
578 Hallegraeff, G. M. (1993). A review of harmful algal blooms and their apparent global increase*.
579 *Phycologia*, *32*(2), 79–99.
580 Hamilton, M. (2011). *Population genetics*. John Wiley & Sons.
581 Haubold, B., & Hudson, R. R. (2000). multilocus data, *16*(9), 847–848.
582 Hu, S., Townsend, D. W., Chen, C., Cowles, G., Beardsley, R. C., Ji, R., & Houghton, R. W.
583 (2008). Tidal pumping and nutrient fluxes on Georges Bank: A process-oriented modeling
584 study. *Journal of Marine Systems*, *74*(1–2), 528–544.
585 Jombart, T. (2008). Adegenet: A R package for the multivariate analysis of genetic markers.
586 *Bioinformatics*, *24*(11), 1403–1405.
587 Keafer, B. A., Churchill, J. H., McGillicuddy, D. J., & Anderson, D. M. (2005). Bloom
588 development and transport of toxic Alexandrium fundyense populations within a coastal
589 plume in the Gulf of Maine. *Deep-Sea Research Part II: Topical Studies in Oceanography*,
590 *52*(19–21 SPEC. ISS.), 2674–2697.
591 Legendre, P., & Andersson, M. J. (1999). Distance-based redundancy analysis: Testing
592 multispecies responses in multifactorial ecological experiments. *Ecological Monographs*,
593 *69*(1), 1–24.
594 Leong, S. C. Y., Murata, A., Nagashima, Y., & Taguchi, S. (2004). Variability in toxicity of the
595 dinoflagellate Alexandrium tamarense in response to different nitrogen sources and
596 concentrations. *Toxicon*, *43*(4), 407–415.
597 Li, Y., He, R., & Manning, J. P. (2014). Coastal connectivity in the Gulf of Maine in spring and

summer of 2004-2009. *Deep-Sea Research Part II: Topical Studies in Oceanography*, *103*, 199–209.

Limeburner, R., & Beardsley, R. C. (1982). The Seasonal hydrography and circulation over Nantucket Shoals. *J. Mar. Res.*, *40*, 371–406.

Maranda, L., Anderson, D. M., & Shimizu, Y. (1985). Toxicity of Gonyaulax tamarensis clones from eastern North American waters. *Toxic Dinoflagellates*, *2*, 349–350.

Martin, J. L., Legresley, M. M., & Gidney, M. E. (2014a). *Phytoplankton monitoring in the Western Isles region of the Bay of Fundy during 2007-2013*. Can. Tech. Rep. Fish. Aquat. Sci.3105.

Martin, J. L., LeGresley, M. M., & Hanke, A. R. (2014b). Thirty years - Alexandrium fundyense cyst, bloom dynamics and shellfish toxicity in the Bay of Fundy, eastern Canada. *Deep-Sea Research Part II: Topical Studies in Oceanography*, *103*, 27–39.

McGillicuddy, D. J., Townsend, D. W., Keafer, B. A., Thomas, M. A., & Anderson, D. M. (2014). Georges Bank: A leaky incubator of Alexandrium fundyense blooms. *Deep Sea Research Part II: Topical Studies in Oceanography*, *103*, 163–173.

MEIRMANS, P. G., & VAN TIENDEREN, P. H. (2004). genotype and genodive: two programs for the analysis of genetic diversity of asexual organisms. *Molecular Ecology Notes*, *4*(4), 792–794.

Nagai, S., Lian, C., Hamaguchi, M., Matsuyama, Y., Itakura, S., & Hogetsu, T. (2004). Development of microsatellite markers in the toxic dinoflagellate Alexandrium tamarense (Dinophyceae). *Molecular Ecology Notes*, *4*(1), 83–85.

Nagai, S., Nishitani, G., Sakamoto, S., Sugaya, T., Lee, C. K., Kim, C. H., … Yamaguchi, M. (2009). Genetic structuring and transfer of marine dinoflagellate Cochlodinium

621 polykrikoides in Japanese and Korean coastal waters revealed by microsatellites. *Molecular*
622 *Ecology*, *18*(11), 2337–2352.
623 Nei, M. (1973). Analysis of Gene Diversity in Subdivided Populations. *Proceedings of the*
624 *National Academy of Sciences*, *70*(12), 3321–3323.
625 Oksanen, J., Blanchet, F. G., Friendly, M., Kindt, R., Legendre, P., McGlinn, D., ... & Stevens,
626 M. H. H. (2016). Package "Vegan"—community ecology package. *R-Package Version 2.4-*
627 *6*.
628 Pettigrew, N. R., Churchill, J. H., Janzen, C. D., Mangum, L. J., Signell, R. P., Thomas, A. C., …
629 Xue, H. (2005). The kinematic and hydrographic structure of the Gulf of Maine Coastal
630 Current. *Deep Sea Research Part II: Topical Studies in Oceanography*, *52*(19–21), 2369–
631 2391.
632 Pilskaln, C. H., Hayashi, K., Keafer, B. A., Anderson, D. M., & McGillicuddy, D. J. (2014).
633 Benthic nepheloid layers in the Gulf of Maine and Alexandrium cyst inventories. *Deep-Sea*
634 *Research Part II: Topical Studies in Oceanography*, *103*, 55–65.
635 Pritchard, J. K., Stephens, M., & Donnelly, P. (2000). Inference of population structure using
636 multilocus genotype data. *Genetics*, *155*(2), 945–959.
637 Raymond, M. (1995). J. Hered. 86:248–249. *J. Hered*, *86*, 248–249.
638 Richlen, M. L., Erdner, D. L., McCauley, L. A. R., Libera, K., & Anderson, D. M. (2012).
639 Extensive genetic diversity and rapid population differentiation during blooms of
640 Alexandrium fundyense (Dinophyceae) in an isolated salt pond on Cape Cod, MA, USA.
641 *Ecology and Evolution*, *2*(10), 2588–2599.
642 Rousset, F., De, S., Montpellier, U., & Bataillon, P. E. (2008). GENEPOP ' 007 : a complete re-
643 implementation of the GENEPOP software for Windows and Linux, 103–106.

644 Rynearson, T. A., & Armbrust, E. V. (2005). Maintenance of clonal diversity during a spring
645 bloom of the centric diatom Ditylum brightwellii. *Molecular Ecology*, *14*(6), 1631–1640.
646 Rynearson, T. a., Newton, J. a., & Armbrust, E. V. (2006). Spring bloom development, genetic
647 variation, and population succession in the planktonic diatom Ditylum brightwellii.
648 *Limnology and Oceanography*, *51*(3), 1249–1261.
649 Sassenhagen, I., Gao, Y., Lozano-Duque, Y., Parsons, M. L., Smith, T. B., & Erdner, D. L.
650 (2018). Comparison of Spatial and Temporal Genetic Differentiation in a Harmful
651 Dinoflagellate Species Emphasizes Impact of Local Processes. *Frontiers in Marine Science*,
652 *5*(October), 1–13.
653 Sjöqvist, C., Godhe, A., Jonsson, P. R., Sundqvist, L., & Kremp, A. (2015). Local adaptation and
654 oceanographic connectivity patterns explain genetic differentiation of a marine diatom
655 across the North Sea-Baltic Sea salinity gradient. *Molecular Ecology*, *24*(11), 2871–2885.
656 Sundqvist, L., Godhe, A., Jonsson, P. R., & Sefbom, J. (2018). The anchoring effect—long-term
657 dormancy and genetic population structure. *The ISME Journal*, *12*(12), 2929–2941.
658 Townsend, D. W., McGillicuddy, D. J., Thomas, M. A., & Rebuck, N. D. (2014). Nutrients and
659 water masses in the Gulf of Maine–Georges Bank region: Variability and importance to
660 blooms of the toxic dinoflagellate Alexandrium fundyense. *Deep Sea Research Part II:*
661 *Topical Studies in Oceanography*, *103*, 238–263.
662 Van Dolah, F. M. (2007). Marine Algal Toxins : Origins , Health Effects , and Their Increased
663 Occurrence Frances M . Van Dolah. *Environmental Health*, *108*, 133–141.
664 Wright, S. (1949). The genetical structure of populations. Annals of Human Genetics. *Annals of*
665 *Human Genetics*, *15*(1), 323–354.
666 Yeh, F. C., Yang, R. C., Boyle, T. B., Ye, Z. H., & Mao, J. X. (1997). POPGENE, the user-

667 friendly shareware for population genetic analysis. *Molecular Biology and Biotechnology*
668 *Centre, University of Alberta, Canada*, *10*, 295–301.
669
670
671
672
673
674
675
676
677

678 Table 1: Sampling dates and number of strains per sample used in this study.

Sample	Date	# of individuals
GBA	5/26	32
GBB	5/28	31
GBC	5/28	33
GBD	5/26	36
GBE	5/30	24
GBF	6/17	30
GBG	6/16	40
GBH	6/24	30
GBI	6/24	30
GBJ	6/23	24
GBK	7/3	19
NSA	5/3	29
NSB	5/20-21	39
NSC	5/28	35
BFA	5/7	28
BFB	5/14	18
BFC	5/24	31
BFD	6/12	38
BFE	6/26	31
BFF	7/2	31
BFG	7/10	20
BFH	7/24	38

679

680

681

682

683

684

685

686

687 Table 2: Environmental data of samples from GoM (obtained from the University of Maine
688 GOMTOX Data Archives http://grampus.umeoce.maine.edu/gomtox/gomtox.htm).

	Nitrate+Nitrite (µM)	Silicate (µM)	Phosphate (µM)	Ammonium (µM)	Temp (℃)	Salinity (psu)	Sigmat (kg m^{-3})	Chlorophyll a (µg L^{-1})	Phaeopigments (µg L^{-1})
GBA	0.10	0.40	0.09	0.20	8.62	32.98	25.59	3.76	0.05
GBB	0.09	0.90	0.10	0.21	9.62	32.97	25.43	2.16	0.32
GBC	1.47	1.22	0.38	0.59	8.17	33.14	25.79	4.61	0.60
GBD	0.15	10.53	0.20	1.35	9.29	33.06	25.55	5.05	0
GBE	0.09	6.83	0.09	0.40	10.62	32.80	25.12	1.82	0.13
GBG	0.09	1.13	0.11	0.72	6.99	31.95	25.02	0.80	0.67
GBH	0.62	0.95	0.10	0.61	11.57	32.81	24.97	2.11	0
GBJ	0.11	1.40	1.22	0.28	11.73	32.38	24.61	0.77	0.03
GBK	0.09	0.03	0.03	0.04	14.04	32.90	24.56	1.48	0.26
BFC	6.63	10.17	0.41	0.16	6.29	29.58	23.24	1.77	0

689
690
691
692
693
694
695
696
697
698
699
700

Table 3: Pairwise comparisons of genotypic differentiation between clusters in GoM. Lower diagonal: F_{ST} values. Upper diagonal: p-values of the Fisher's exact test. Bold characters denote significance at α=0.05 after Bonferroni correction.

	Southern cluster	Northern cluster	Mixed cluster
Southern cluster	--	**Highly sign.**	**Highly sign.**
Northern cluster	**0.051**	--	**Highly sign.**
Mixed cluster	**0.061**	**0.088**	--

Table 4: Number of strains per sub-clusters (N), number of different clonal lineages (G), overall clonal diversity (G/N), allele diversity calculated with all strains (H_t) and excluding replicated genotypes (Ht unique).

	N	G	G/N	G (N=59)	G/N (N=59)	H_t	Ht (unique)
GB-Southern	212	72	0.34	27	0.46	0.49	0.63
GB-Mixed	86	45	0.52	37	0.63	0.55	0.64
GB-Northern	31	19	0.61	19	N/A	0.52	0.5
BoF-Southern	59	35	0.59	35	0.59	0.47	0.59
BoF-Mixed	18	13	0.72	13	N/A	0.50	0.53
BoF-Northern	158	62	0.39	30	0.51	0.51	0.63
NS-Southern	103	43	0.42	33	0.56	0.45	0.59

751 **Figure Legends**

752

753 Figure 1. The location of samples in GoM. Sampling sites are indicated with black dots/circle.
754 GB's location is shown in dashed outline, arrow lines indicate the Main Coastal Current (MCC)
755 and GB gyre.

756 Figure 2: Principal Component Analysis (PCA) of a covariance matrix from the genetic data of
757 **GoM**. Both axes are significant: Axis 1: percent inertia=38%, F_{ST} =0.030, p=0.004; Axis 2:
758 percent inertia=30%, F_{ST} =0.024, p=0.000. Shapes correspond to the genetic clusters suggested
759 by the AMOVA analyses (Circles=Southern Cluster; Stars=Northern Cluster; Squares=Mixed
760 Cluster).

761 Figure 3: Population structure of **GoM** determined by Bayesian cluster analysis. Results of
762 STRUCTURE analysis are presented for K=3. Dashed lines separate samples from different sub-
763 regions in GoM. Colors of sample names correspond to the genetic clusters suggested by the
764 PCA & AMOVA analyses (Orange=Southern Cluster; Blue=Northern Cluster; Yellow=Mixed
765 Cluster).

766 Figure 4: Environmental association analysis based on distance-based Redundancy Analysis
767 (dbRDA). RDA plot for significant environmental factors (silicate, P=0.0068; nitrate+nitrite,
768 P=0.0007). Colors correspond to the clusters suggested by the STRUCTURE analyses
769 (Orange=Southern Cluster; Blue=Northern Cluster; Yellow=Mixed Cluster).

770

771

772

773

774

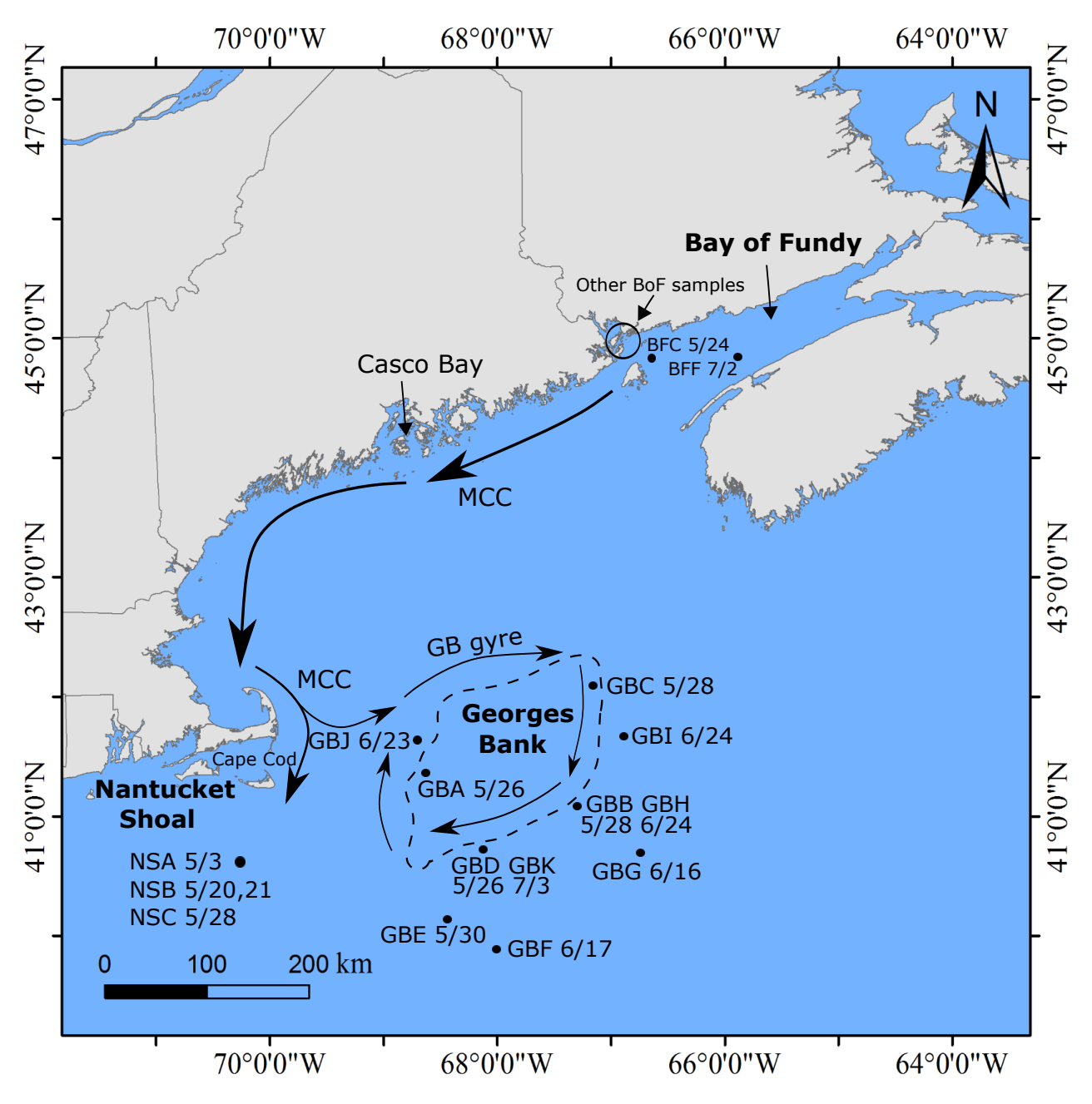
70°0'0"W
68°0'0"W
66°0'0"W
64°0'0"W
47°0'0"N
45°0'0"N
43°0'0"N
41°0'0"N
N
Bay of Fundy
Other BoF samples
BFC 5/24
BFF 7/2
Casco Bay
MCC
GB gyre
MCC
GBC 5/28
Georges Bank
GBI 6/24
GBJ 6/23
Cape Cod
GBA 5/26
Nantucket Shoal
GBB GBH 5/28 6/24
NSA 5/3
NSB 5/20,21
NSC 5/28
GBD GBK 5/26 7/3
GBG 6/16
GBE 5/30
GBF 6/17
0
100
200 km

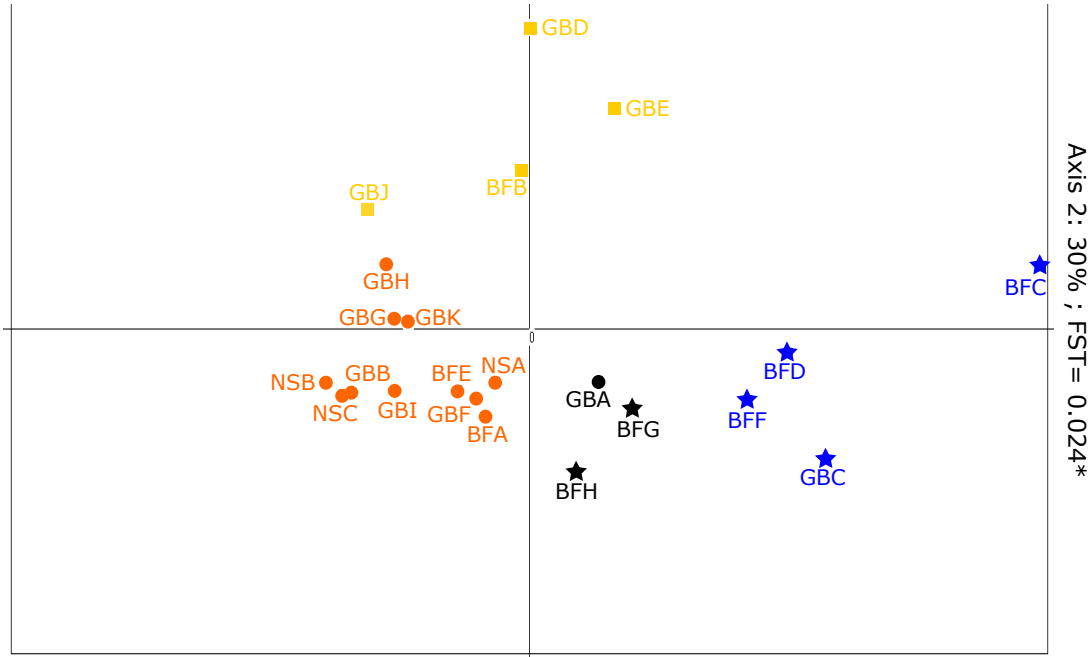
GBD
GBE
GBJ
BFB
GBH
GBG
GBK
BFC
0
NSB
GBB
BFE
NSA
NSC
GBI
GBF
BFA
GBA
BFG
BFD
BFF
BFH
GBC
Axis 2: 30% ; FST= 0.024*
Axis 1: 38% ; FST= 0.030*

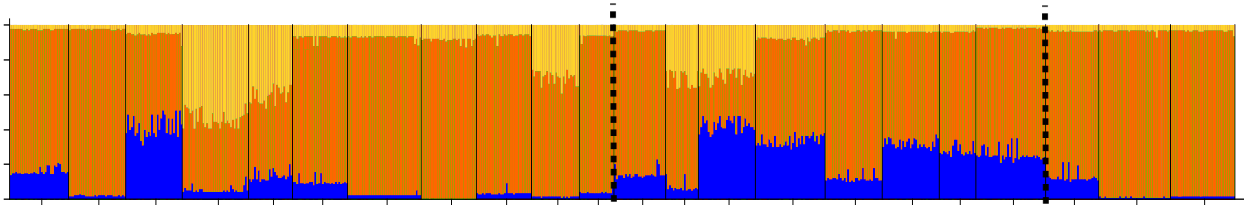
1.00
0.80
0.60
0.40
0.20
0.00
GBA
GBB
GBC
GBD
GBE
GBF
GBG
GBH
GBI
GBJ
GBK
BFA
BFB
BFC
BFD
BFE
BFF
BFG
BFH
NSA
NSB
NSC

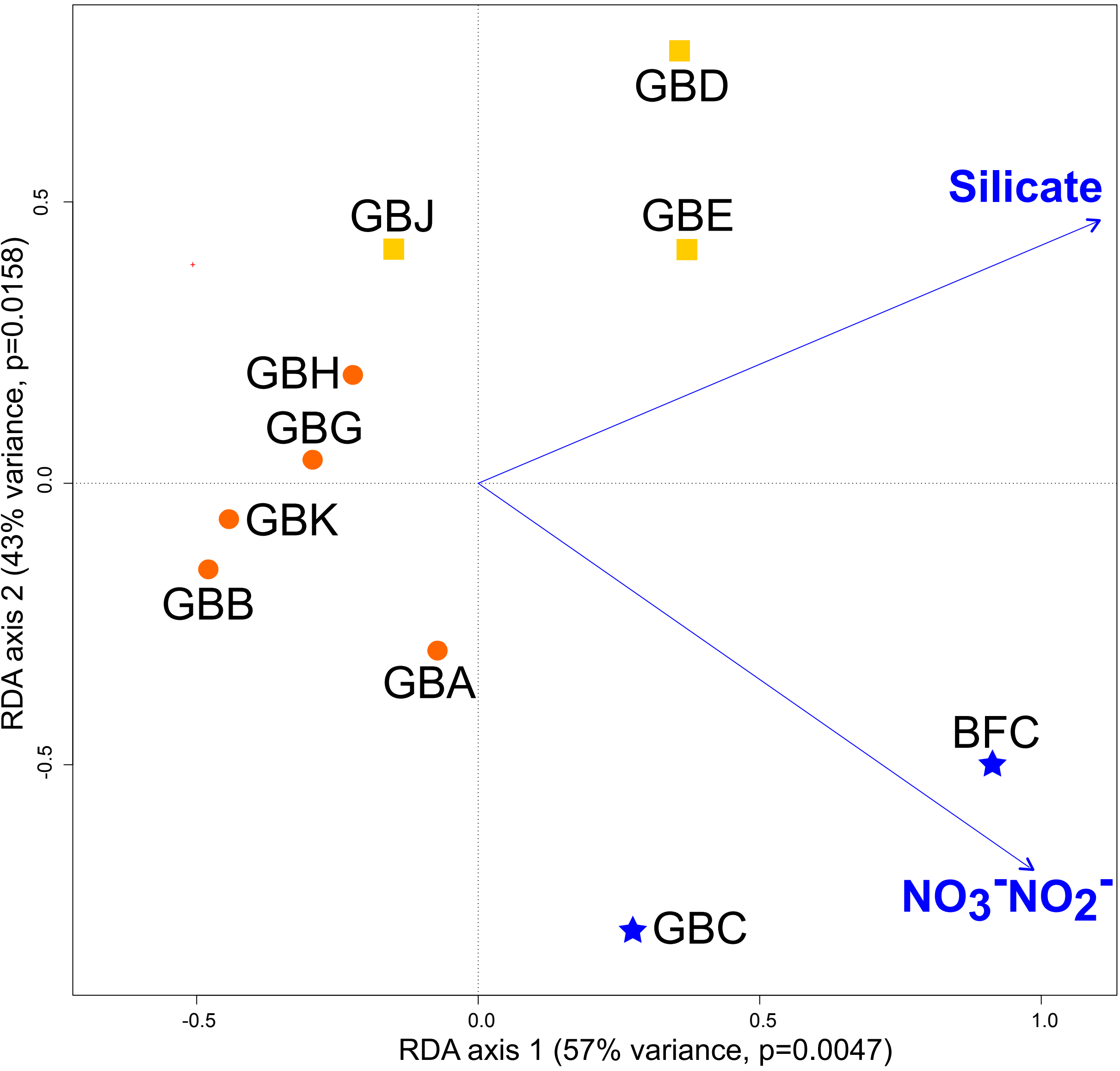
GBD
GBJ
GBE
Silicate
GBH
GBG
GBK
GBB
GBA
BFC
GBC
NO3-NO2-
0.5
0.0
-0.5
-0.5
0.0
0.5
1.0
RDA axis 2 (43% variance, p=0.0158)
RDA axis 1 (57% variance, p=0.0047)